PHILOSOPHICAL TRANSACTIONS B

Phil. Trans. R. Soc. B.
doi:10.1098/RSTB-2019-0527

Non-stomatal processes reduce gross primary productivity in temperate forest ecosystems during severe edaphic drought

Louis Gourlez de la Motte[1i], Quentin Beauclaire[1], Bernard Heinesch[1], Mathias Cuntz[2], Lenka Foltýnová[3], Ladislav Šigut[3], Natalia Kowalska[3], Giovanni Manca[4], Ignacio Goded Ballarin[4], Caroline Vincke[5], Marilyn Roland[6], Andreas Ibrom[7], Denis Lousteau[8], Lukas Siebicke[9], Bernard Longdoz[1]

[1]University of Liège – Gembloux Agro-Bio Tech, Terra Teaching and Research Center, Belgium
[2]Université de Lorraine, AgroParisTech, INRA, UMR Silva, 54000 Nancy, France
[3]Global Change Research Institute CAS : Brno, Moravian region, CZ
[4]European Commission, Joint Research Centre (JRC), Ispra, Italy.
[5]Earth and Life Institute, UCLouvain
[6]University of Antwerp, Plants and Ecosystems, Universiteitsplein 1, 2610 Wilrijk, Belgium
[7]Technical University of Denmark (DTU), Department of Environmental Engineering, Bygningstorvet 115, DK 2800 Lyngby, Denmark
[8]INRA, UMR ISPA, Villenave d'Ornon, F-33140.
[9]Bioclimatology, University of Goettingen, Büsgenweg 2, 37077 Goettingen, Germany
[i]louis_delamotte@hotmail.com;

Keywords: drought, model, stomatal conductance, forest, photosynthesis, eddy covariance

Summary

Severe drought events are known to cause important reductions of gross primary productivity (*GPP*) in forest ecosystems. However, it is still unclear whether this reduction originates from stomatal closure (Stomatal Origin Limitation) and/or non-stomatal limitations (Non-SOL). In this study, we investigated the impact of edaphic drought in 2018 on *GPP* and its origin (SOL, NSOL) using a data set of 10 European forest ecosystem flux towers. In all stations where *GPP* reductions were observed during the drought, these were largely explained by declines in the maximum apparent canopy scale carboxylation rate $V_{CMAX,APP}$ (NSOL) when the soil relative extractable water content dropped below around 0.4. Concurrently, we found that the stomatal slope parameter (G_1, related to SOL) of the Medlyn et al. unified optimization model linking vegetation conductance and *GPP* remained relatively constant. These results strengthen the increasing evidence that NSOL should be included in stomatal conductance/photosynthesis models to faithfully simulate both *GPP* and water fluxes in forest ecosystems during severe drought.

*Author for correspondence (louis_delamotte@hotmail.com).
†Present address: Gembloux Agro-Bio Tech, Avenue de la faculté 2, 5030 Gembloux, Belgique

1 Introduction

With global climate change, droughts are likely to be more intense [1,2]. In 2018, a severe drought event occurred in Northern and central Europe causing forest fires, crop yield losses [3]. Europe experienced major reduction of gross primary productivity (*GPP*) and transpiration (E) similarly to previous extreme events such as the 2003 Europe drought-heatwave [4] mostly because of soil water limitation [5,6]. Continuous measurements of ecosystem CO_2 and water fluxes captured throughout Europe at eddy covariance flux tower stations thus provide a great large scale "natural experiment" to study the impact of drought on GPP and E [7].

There is increasing evidence that *GPP* reductions due to droughts could originate from both changes in stomatal behavior (stomatal origin limitation, SOL) and non-stomatal traits (non-stomatal origin limitation, NSOL) [8–12]. Proposed NSOL mechanisms are reduced Rubisco activity (carboxylation rate) and/or electron transport activity [13], reduced active leaf area index [13], reduced mesophyll conductance (including the intercellular airspace, cell walls, plasma membranes, cytoplasm, and the chloroplast envelopes [14], g_m) [15] or a combination of those [11,16]. The cause for *GPP* reduction is still subject to debate [17,18] and the modelling of SOL and NSOL and their (de)coupling is still poorly constrained by data. As a result, there is a strong need to examine if different mechanisms are relevant and if models could be improved by developing more evidence-based functions for the impact of drought stress [19,20].

In leaf/canopy photosynthesis models, gross primary assimilation (A) is very often modelled using the Farquhar et al., [21] photosynthesis model for C3 species [9,10,13]. In this model, Rubisco limited photosynthesis (usually close to light saturation) is a function of the maximum carboxylation rate (V_{cmax}) and the internal CO_2 leaf concentration (C_i) which implicitly considers that C_i is equal to the CO_2 concentration in the chloroplasts (C_c). As C_i cannot be measured directly, it is usually approximated by employing Fick´s diffusion law through the stomata using a stomatal conductance (g_s). This representation requires the determination of stomatal conductance by modelling. In this study, following [10], we use the concept of apparent V_{cmax} ($V_{cmax,app}$) recognizing that variations in $V_{cmax,app}$ can result of either from changes in the actual maximum rate of carboxylation or from changes in g_m which are not explicitly represented in this diffusion model. Consequently, when drought occurs, it impacts directly stomatal behavior (closure) and then photosynthesis by limiting the diffusion of CO_2 into the leaf which results in reduced C_i (SOL) or/and it impacts non-stomatal mechanisms (NSOL) which result in decreases of $V_{cmax,app}$ [10,20].

A long standing model stomatal conductance model from [22] states that stomata should act to maximize carbon gains while minimizing water losses (transpiration, E) that is to maximize the integrated sum of $A–E$ where λ (mol C mol^{-1} H_2O) is the carbon cost of water gain $\frac{\partial A}{\partial E}$ or marginal water use efficiency [23] (note that we inverted the original expression). Medlyn et al., [24] proposed a reconciliation of the optimal stomatal behavior theory [22] with empirical stomatal models linking g_s and A. Their work resulted in a unified stomatal optimization model (USO) with a form similar to former empirical expressions [25,26] (see Eq.3) where the slope between g_s and $A*f$ (g_1) is a key parameter (called the stomatal slope parameter). g_1 is directly interpretable as inversely related to λ and to intrinsic water-use efficiency (iWUE, A/g_s) normalized by vapor pressure deficit (VPD) and CO_2 air concentration (C_a) [27].

The USO model has been used both at the leaf level using leaf gas exchange data [28] and at the ecosystem level using eddy covariance flux observations [29] during non-water limited periods. During water limited periods, various responses of g_1 (leaf level, SOL) to soil moisture was found [10] for a large range of species while a more consistent pattern of decreasing $V_{cmax,app}$ was found. In a recent work, a good correlation between leaf scale and ecosystem scale $g1$ (or G_1) response to soil moisture was found in a woodland dominated by Acacia trees thereby demonstrating the ability of both leaf and ecosystem scale approaches to quantify drought effect [30].

In this study, we used the USO model combined with the Farquhar C_3 model (considering that C_i = C_c) to study the origin of edaphic drought impacts on *GPP* (SOL and/or NSOL) in forest ecosystems using eddy covariance (EC) flux measurements by replacing leaf level variables by their ecosystems analogs using a big leaf framework [27,31]. The surface conductance (G_s analogous to g_s) was

estimated by inverting the Penman-Monteith equation [32]. We then inferred the bulk stomatal slope parameter (G_1 analogous to *g1*) and the maximum apparent carboxylation rate of the ecosystem ($V_{CMAX,APP}$) [33] at a daily time step for each ecosystem. The study was restricted to the growing period excluding any autumn senescence or spring leaf emergence influence on the variation of $V_{CMAX,APP}$.

In addition, drought intensity was quantified using the relative extractable water (*REW*) as proposed by [5] which is a normalized index of soil water deficit varying from 0 to 1 which allows for edaphic status inter-site comparisons. This index was used in previous studies [5,34] and, based on their results, we hypothesize that both *E* and *GPP* reductions will occur when *REW* fell below ≈0.4.

The objective of this work is to examine the response of G_1, as a measure for SOL, and $V_{CMAX,APP}$, as a measure for NSOL to soil water deficit using EC data collected in forests during the 2018 European drought. More specifically, we intend to answer the following questions: (1) how was *REW* impacted by the drought in forest sites in 2018? (2) Can we confirm the *REW* threshold of ≈0.4 for *GPP* reductions found in previous studies [5,34]? (3) To what degree did SOL and NSOL impact *GPP* during the drought? (4) What were G_1 and $V_{CMAX,APP}$ responses to *REW* functions shapes and how did these responses vary across sites?

2 Material and methods

2.1 *Site and data description*

Data have been processed by the Ecosystem Thematic Centre of the Integrated Carbon Observation System (ICOS) and form the 2018 drought ICOS/Fluxnet data set [35] which is a compilation of eddy covariance fluxes, meteorological and edaphic data during the 2018 European drought at half hourly resolution. Only sites with a sufficiently resolved vertical profile of soil water content sensors were selected. The main site characteristics are summarized in Table 1. Flux data followed the standard FLUXNET processing [36], including friction velocity (u_*) filtering [37] and *GPP* determination by nighttime flux partitioning [38]. Only data marked with highest quality flags were used for this study. Latent heat fluxes were not corrected for energy balance closure.

2.2 *Quantification of drought*

The intensity of edaphic drought was quantified by computing the relative extractable water content (*REW*) [5] at each time step and for the entire root depth using:

$$REW = \frac{\sum_i \frac{SWC_i - SWC_{WP,i}}{SWC_{FC,i} - SWC_{WP,i}} \Delta h_i}{h_{max}} \quad (1)$$

where *i* is the index of each soil layers over the rooting depth, SWC_i is the actual soil water content, SWC_{WP} is the soil water content at the wilting point, SWC_{FC} is the soil water content at field capacity, Δh is the thickness of each layer and h_{max} is the maximum rooting depth. Each soil horizon was divided into soil layers corresponding to the number of sensors installed in the horizon. The layer boundaries were the horizon limits or the midway point between two sensors. Soils related data are summarized in the supplements (Table S1). For each layer, SWC_{WP} and SWC_{FC} were estimated using soil retention curves based on either measurements (by research teams) or modeling (based on soil textures) and checked for consistency with SWC 48 hours after a rain event for SWC_{FC} and with minimum SWC values observed at the site for SWC_{WP} to avoid negative *REW* values. When not available, the maximum depth was defined as the bedrock depth [5]. When data were available (BE-VIE and BE-BRA), *REW* was corrected for the coarse fraction by applying a correction factor for each layer. According to [5,34] it's expected that both *GPP* and G_s start do decrease when *REW* drops below ≈0.4. The evolution of REW at each site in 2018 is presented in the supplements (Figure S1).

2.3 *Canopy surface variables*

Detailed computation procedures for canopy surface variables are fully described in [31]. First the aerodynamic conductance to water transfer (G_{aw}) was computed as a combination of an aerodynamic conductance to momentum (1st term) and a boundary layer conductance (2nd term) as follow:

$$G_{aw} = \frac{u_*^2}{u(z)} + (6.2u_*^{-0.67})^{-1} \quad (2)$$

where u_* is the friction velocity (m s^{-1}), and u(z) the wind speed at measurement height (z). Canopy surface conductance for water (G_s, m s^{-1}) was computed by inverting the Penman-Monteith equation [32]:

$$G_s = \frac{LEG_{aw}\gamma}{s(R_n - G - S) + \rho C_p C_a VPD_a - \lambda E(s+\gamma)} \quad (3)$$

where *LE* is the latent heat flux (W m^{-2}), γ is the psychrometric constant (Pa K^{-1}), s is the slope of the saturation vapor pressure curve at air temperature (Pa K^{-1}), R_n is the net radiation (W m^{-2}), *G* is the ground heat flux (W m^{-2}), S is the sum of all storage terms (W m^{-2}), C_p is the heat capacity of dry air (1005 J kg^{-1} K^{-1}) and VPD_a is the vapor pressure deficit of ambient air (Pa). G was considered negligible when not available while S was not available and was set to 0 at all sites.

The CO_2 concentration at the canopy surface (C_s), needed in the USO and diffusion equations, was computed as:

$$C_s = C_a + \frac{NEE}{\frac{G_{aw}}{1.32}} \quad (4)$$

where C_a (µmol CO_2 mol^{-1}) is the CO_2 air concentration at the measurement height, NEE (µmol CO_2 m^{-2}) is the net CO_2 ecosystem exchange and the factor 1.32 is the ratio of diffusivities of CO_2 and water vapor in the boundary layer. The vapor pressure deficit at the canopy surface (*VPD*s, Pa) was also computed (see [31] for more details). G_s is a good predictor of bulk stomatal conductance only when evaporation is small compared to transpiration, data collected during a period of 48 hours following a rain event were discarded. Secondly, the analysis was restricted to the growing season; avoiding senescence and leaf emergence periods. We defined this period as the days when the daily *GPP* (average over all the available years) smoothed with a 15 days moving average window was higher than 70% of the 95th percentile of the daily *GPP* distribution. G_s data were also filtered excluding half hour with LE<0 or R_n<0. Negative G_s values were filtered and G_s outliers were also discarded by removing data when G_s were higher than the 98th percentile of the G_s distribution.

2.4 *Stomatal origin limitations*

Similarly to previous work [10,39], reductions of *GPP* originating from SOL were assessed by analyzing dependence on *REW* of the G_1 parameter used in the USO model developed by [24] but adapted to the ecosystem scale using bulk ecosystem parameters [27]:

$$G_s = G_0 + 1.6\left(1 + \frac{G_1}{\sqrt{VPD_s}}\right)\frac{GPP_{high}}{C_s} \quad (5)$$

where, GPP_{high} is the *GPP* at high radiation (Rg>500 W m^{-2}) replaces net assimilation in the original leaf scale expression of the model, G_s replaces stomatal conductance and leaf surface variables were replaced by their corresponding canopy surface values [40] (C_s the air CO_2, VPD_s). In this expression, the nocturnal stomatal conductance G_0 was set to 0 as its magnitude can be considered negligible when compared to the other terms at saturating daylight conditions [27]. G_1, the slope parameter, is a physiologically meaningful parameter as it was shown to be inversely related to λ [24] and to iWUE [27].

G_1 was obtained by inverting equation 5 using half-hourly measurements. Because leaf respiration was neglected in equation 5, the equation was inverted only for high radiation data so that GPP_{high} should much higher than leaf respiration. Negative G_1 values were filtered and outliers were also discarded by removing data when absolute G_1 was 2 times higher than the average absolute deviation from the median. Finally, daily G_1 averages were then computed for days with at least 5 valid half-hourly values.

The response of G_1 to *REW* was fitted with a segmented linear response curve (2 segments) in order to test the presence of a *REW* threshold (break-point) above which G_1 is constant ("no effect range") and under which stomatal regulation occurs (G_1 decreases or increases) [41]. After a first fit, outliers were removed by exclusion of the G_1 value having absolute residuals more than 2.2 times the standard deviation of the residuals distribution. A second fit was then done. Parameters obtained from a second fit were G_1*, i.e. the average G_1 value within the "no effect range", the break point *REW* value ($REW_{B,G1\ I}$) and the slope/intercept of the G_1 decrease/increase. The presence of the break point was further tested by comparing the residuals of the model to those of a simple linear regression model using a F-test.

2.5 *Non stomatal origin limitations*

Reductions of *GPP* originating from NSOL were studied by assessing the effect of water stress on apparent bulk V_{cmax} hereafter called $V_{CMAX,APP}$. It was obtained by inverting the expression of Rubisco-limited photosynthesis during high radiation conditions [21]:

$$V_{CMAX,APP} = \frac{GPP_{high}(C_i + K_m)}{(C_i - \Gamma^*)} \quad (6)$$

where $V_{CMAX,APP}$ is expressed per m^2 of soil and not of leaf as usual. K_m is the effective Michaelis Menten coefficient kinetics and Γ* is the CO_2 compensation point which were h both computed using

temperature responses following [42], GPP_{high} is the *GPP* at Rg>500 W m^{-2} while C_i was computed using the Fick´s diffusion law [43]:

$$C_i = C_s - \frac{GPP_{high}}{\frac{G_s}{1.6}} \quad (7)$$

Note than in equation 5, 6 and 7, leaf respiration was neglected which should have a small effect on the results as, at high radiation, leaf respiration should be much smaller than *GPP*. Half hourly values of $V_{CMAX,APP}$ were then normalized for temperature to 25°C using an Arrhenius equation [31] fitted for each decile of *REW* as $V_{CMAX,APP}$ response to temperature was found to decrease under drought conditions. Finally, $V_{CMAX,APP}$ was averaged on a daily basis and days with less than 5 half-hourly values were discarded. Considering the way we estimated $V_{CMAX,APP}$, a decrease in $V_{CMAX,APP}$ indicates NSOL of *GPP* including either changes in mesophyll conductance or in actual V_{CMAX} or other processes limiting *GPP* (apart from stomatal closure). The response of $V_{CMAX,APP}$ to *REW* was assessed using the same segmented linear regression model as explained in the previous section. $V_{CMAX,APP}$* and $REW_{B,VCMAX}$ were defined as the average of $V_{CMAX,APP}$ values (normalized at 25°C) within the no effect range and the break point *REW* value respectively.

2.6 *Degree of SOL and NSOL*

To illustrate the degree of SOL and NSOL due to edaphic drought, following [10], a sensitivity analysis was performed to explore the impact of drought-induced changes in G_1 and $V_{CMAX,APP}$ on *GPP*. The impact of NSOL was assessed by comparing measured *GPP* to a theoretical non affected value corresponding to a "modelled" *GPP* computed using inverted Eq. 5 with $V_{CMAX,APP}$* instead of $V_{CMAX,APP}$ and a C_i obtained from Eq 6 using observed G_s values (Eq. 2) and measured *GPP* values. Similarly, the impact of SOL was assessed by comparing measured *GPP* to "modelled" unaffected *GPP* computed using constant G_1* values and observed $V_{CMAX,APP}$ values. The degree of limitation (DoL) was computed as the ratio of modelled "unaffected" *GPP* against measured *GPP* and represents the factor by which *GPP* was divided because of SOL or NSOL.

3 Results

3.1 G_s *and* GPP_{high}

GPP_{high} and G_s (for Rg>500) normalized by their respective maximum values in relation with *REW* are presented in Figure 1. At all sites, we can observe that both GPP_{high} and G_s behave similarly. High values of both GPP_{high} and G_s were observed for high *REW* while both variables decreased simultaneously with *REW*. There was an exception at BE-Vie where such pattern was not observed although both variables still behaved similarly. The lowest GPP_{high} and G_s values were observed at sites such as CZ-Raj, FR-Bil and DE-Hai where very low *REW* values (lower than 0.15) were reached. At IT-Sr2, G_s and GPP_{high} were still quite high (around half of maximum values) even for very low *REW* values most probably because, in this sandy soil, rooting depth was probably deeper than the deepest available SWC sensor (1.2 m, see Table S1 in supplements) which caused an underestimation of *REW*.

3.2 *Response of* G_1 *to edaphic drought*

G_1 was found constant at all sites apart from DE-Hai and even for sites where *REW* values lower than 0.4 were observed (Figure 2). In BE-Bra G_1 seems to enhance at low *REW* but the segmented model did not perform significantly better than the linear one. In DE-Hai, G_1 was found to increase when *REW* dropped below a very low value of 0.15 which is quite close to the wilting point. Such low *REW* were also observed during the growing season at CZ-Raj and IT-SR2 but no similar behavior was observed. The lowest G_1*(1,6 $kPa^{0.5}$ at CZ-Raj) was more than three times lower than the highest value (5.1 $kPa^{0.5}$ at FR-Bil, Table 2).

3.3 Response of $V_{CMAX,APP}$ to edaphic drought

The effect of NSOL caused by drought was studied by analyzing the dependence of the temperature normalized $V_{CMAX,APP}$ values on *REW* (Figure 3). At all sites that experienced low *REW* conditions (below ≈ 0.4) apart BE-Vie and IT-Sr2, constant $V_{CMAX,APP}$ were observed for large *REW* values followed by a decrease when *REW* declined below a $REW_{B,VCMAX}$ threshold. The $REW_{B,VCMAX}$ were not significantly different (according to the confidence intervals) than the value of 0.4 which was found in previous studies with an exception at DK-Sor where $REW_{B,VCMAX}$ was higher ($REW_{B,VCMAX}$=0.85±0.09, Table 2). The high $REW_{B,VCMAX}$ observed at DK-Sor might result from an overestimation of *REW* as the shallowest available SWC probe was at 15 cm depth (see Table S1 in supplements) and was not able to catch the beginning of the progressive drying of the upper layers that contain a large amount of roots. The most impacted site was DE-Hai where *REW* almost reached the wilting point (*REW* ≈ 0) and very low $V_{CMAX,APP}$ values (≈15 µmol m^{-2} s^{-1}) probably because of shallow soil and rooting depth (0.6 m).

3.4 *Degree of stomatal and non-stomatal limitation*

DoL reached values of 5 for NSOL at DE-HAI while it remained close to 1 for SOL at all sites (Figure 4). This analysis therefore confirms that, at all sites, NSOL were the dominant mechanism. As a result, reducing $V_{CMAX,APP}$ while maintaining G_1 constant could capture the variations of both GPP_{high} and G_s with drought (identical conclusions are obtained if we focus the analysis on G_s instead of *GPP*, data not shown). It is also worthwhile noticing that the increasing G_1 observed at DE-Hai (and at BE-Bra in a lesser extent) did not lead to important changes in *GPP*.

4 Discussion

4.1 *Methodological limitations*

Although the responses of $V_{CMAX,APP}$ and G_1 to *REW* were relatively consistent, some sites showed unexpected behaviors. For example, $REW_{B,VCMAX}$ at DK-Sor was much higher than expected (0.85) because some SWC sensors experienced failures during the drought. At IT-Sr2, no limitation of *GPP* was found although very low *REW* values were estimated probably because the SWC sensor profile was not deep enough to capture the whole rooting depth. Multiple and deeper sensor profiles (with matching wilting points and field capacities) would certainly help to reduce these uncertainties. Complementary measurements such as predawn leaf water potential and soil matric potential [17,44], when *REW* approaches values close to 0.4 at the site would also be useful.

The big leaf approach used in this study also has several limitations [31] which could be critical when comparing leaf scale derived parameters to big leaf canopy scale estimates [27,29,31] or when attributing a behavior to a specific specie. First, the approach is only able to derive bulk parameters and is unable to distinguish the vertical and horizontal distribution of the properties. Horizontal heterogeneity is especially crucial at mixed forest sites where different species could show different responses to drought (and different root depth and therefore REW) which would blur their respective responses in the measured signal. This especially critical at BE-Vie where the two most frequent wind directions (South-West and North-East) correspond to different stands (coniferous and beech stands) with possibly different root depth, REW and weather conditions [45]. Separating the data between each sector did not however improve the relation because of the lack of data (data no shown).

At sites with dense canopy and high leaf area index (LAI), vertical gradients of the parameters (G_s, G_1 and $V_{CMAX,APP}$) could result from vertical gradients within plants of the same species or from physiological differences across species [27]. Sun leaves, developed under high irradiance, usually exhibits higher WUE (lower G_1) than those developed under shady conditions [46] primarily because of higher photosynthetic capacities. However, more critical for this study, little is known on which degree these vertical gradients (within and across species) could affect the response of G_1 and $V_{CMAX,APP}$ to drought. To our knowledge, in most Earth system models, the same reduction functions of photosynthesis during edaphic drought (either NSOL or SOL) are used for sun and shade leaves [17]. More complex multiple layers and/or sun-shade models as well as additional data gathered at multiple canopy layers would be needed to assess this question more closely.

Moreover, soil and vegetation components cannot be distinguished so that critical variables such as G_s (and variables depending on it as G_1 and C_i) will inevitably contain some signal from the soil. This signal can be reduced by filtering the data after rain events [27] and should be small for dense canopies with LAI higher than 2-3 [47] (which is the case all sites) and even smaller when the upper soil layer dries.

Finally, systematic errors (energy balance non-closure [48]) in EC fluxes are also major sources of uncertainties that affects G_1 and $V_{CMAX,APP}$ magnitudes. However it was found that, at multiple flux tower sites, the surface energy balance was not modified during the 2018 drought [49]. This source of error is therefore unlikely to affect G_1 and $V_{CMAX,APP}$ responses do REW.

Nevertheless, despite all the limitation the big leaf approach detailed above, this framework was very suitable for this multi-site study as it relied on very few ancillary data [31]. If the comparison of G_1 and $V_{CMAX,APP}$ (which inherently has a different meaning than leaf level $V_{cmax,app}$) is not straightforward, analyzing the dynamics of these parameters inferred from *in situ* EC data during drought provides very useful information about how forest ecosystems reacted to these events.

4.2 *Implications of NSOL for the modeling of* GPP *and transpiration*

In this study, similarly to [5], we found that *GPP* and G_s reductions can be expected when *REW* drops below ≈0.4. To account for these reductions, using empirical reduction factors (ranging from 1 to 0) when soil water content falls below a given threshold is a widely used approach [17]. However,

it is questionable whether the reduction factors should be applied to SOL and/or to NSOL. This was previously investigated in Mediterranean ecosystems [8,13,50] and it was found that, calibrating the model on either *GPP* or transpiration (*E*) (not both) by considering only SOL during edaphic drought conditions systematically led to overestimates of WUE which did not allow to correctly simulate both fluxes. Surprisingly, it was found that applying NSOL only was sufficient to correctly simulate both *GPP* and *E*.

In this study, we found that reducing $V_{CMAX,APP}$ when *REW* dropped below ≈0.4 and using a constant G_1 parameter (from the USO model [24]) allowed to capture both *GPP* and G_s reductions at European forest sites. Similar conclusions were also found by [51] in four different ecosystems (temperate grassland, tropical savanna, boreal and one temperate forest). More specifically, relatively consistent behavior was observed at the three beech (*Fagus Sylvatica*) forest sites (FR-Hes, DK-Sor and DE-Hai) where NSOL were the main source of photosynthesis reductions with relatively constant G_1. Similarly, in a study carried on adult beech using leaf level measurements, the Ball-Berry slope was found almost insensitive to soil water potential [52]. Our results are in agreement with [5] who observed constant WUE even for very low REW during the 2003 drought and with [53] who also found unchanged annual iWUE derived from tree ring carbon isotopic composition.

Studies were also performed at the leaf scale to study the impact of drought on NSOL and SOL. In their meta-analysis, [10] found highly variable responses of g_1 (leaf level) for woody species ranging from rather constant to severely decreasing g_1 with drought. Decreasing $V_{cmax,app}$ (NSOL) were however found for all species. It was also highlighted that NSOL was the main factor limiting photosynthesis under severe stress in ten Mediterranean herbs and shrubs species [11,54] and, more importantly for this study, for four tree species [20]. Unfortunately, a direct comparison with our results cannot be carried out as the studied species were different. Such direct comparison have been carried out in a woodland dominated by Acaccia trees by [30] who found a close agreement between G_1 and g_1 estimated from ecosystem (EC big leaf) and leaf level approach respectively.

According to [55], NSOL could be caused by the variations of a finite mesophyll conductance with soil water availability [56] which, if not taken into account, leads to wrong estimates of actual V_{cmax} [57] (which was implicitly taken into account by using $V_{CMAX,APP}$). In addition, the hypothesis that, under severe droughts, *GPP* can be directly impacted by biochemical limitations which cause the reduction of actual V_{CMAX} should not be discarded [58]. Separating NSOL between these two mechanisms (mesophyll conductance and actual V_{CMAX}) was not done in this study. Currently, without addition leaf level data to better understand the mechanisms underlying mesophyll conductance changes during droughts, the use of an apparent $V_{CMAX,\,APP}$ [15,17,20].

4.3 *Optimal stomatal behavior during drought and iWUE*

We did not find a general pattern of systematically decreasing G_1 during drought or, in other words, an increasing iWUE for stomatal closure (increasing λ) across ecosystems as theoretically predicted [23,59]. In contrary, we found constant G_1 (and therefore λ) values at most sites and even increasing values at DE-Hai (and BE-Bra in a lesser extent). This result (a constant G_1) is rather surprising as it would suggest that changes in stomatal conductance responses were not needed to model G_s under long term water stress events [50] and that λ does not increase with drought. We argue that this is caused by the fact that NSOL were not considered by [23,59] in their analysis as stomatal closure (reduced G_s) is known to regulate leaf water flows in response to soil water availability [60] as, without such mechanisms, leafs would be quickly dehydrated. However, one should consider that stomatal closure in response to drought does not necessarily lead to a decrease in G_1 as, in USO, any reduction of $V_{CMAX,APP}$ lead to a reduction in stomatal conductance [10]. At very low REW values, previous studies showed that C_i could even increase because of NSOL [61] which would explain the increase of G_1 we observed at DE-Hai.

Another more complex approach to stomatal conductance modeling is to model stomatal conductance in function of leaf water potential which is expected to regulate G_s [62]. This approach requires a complete model of water flow from the soil through the plant to the atmosphere [63]. This kind of model was tested by reducing the stomatal slope of the Ball-Berry-Leuning model [26] with leaf water potential but the model did not account for NSOL [44]. Recently, [64] proposed a new

optimization model in which, stomatal behavior maximizes photosynthesis and where the costs of stomatal closure arise from NSOL (mesophyll conductance and/or carboxylation rate) and/or loss of hydraulic conductance [65]. This results in a parameter, equivalent to G_1, which is expressed as a function of measurable variables such as hydraulic conductivity, leaf water potential and V_{cmax}. This model has been successfully tested on saplings for different plant functional types [66] and fitted well sub-daily leaf scale observations but this still needs to be tested for longer term *in situ* ecosystem droughts. This could not be done in this study as leaf and soil water potentials were lacking. It does, however, highlight a promising research path for the future.

5 Conclusion

In this study, we used a big leaf framework to investigate the origin of edaphic drought impacts on *GPP* (stomatal origin limitation and non-stomatal origin limitation) in European forest ecosystems during the 2018 drought. In agreement with [5], we found that *GPP* and G_s were both greatly affected by soil moisture depletion at many sites. We went a step further by showing that these reductions could be faithfully modelled by decreasing $V_{CMAX,APP}$ (NSOL) when the *REW* dropped below around 0.4 while keeping the G_1 (SOL) parameter from the USO model [24] constant. These results were rather unexpected as it would suggest that stomatal closure was not responsible for *GPP* reductions with drought. We argue that this was caused by the fact that G_1 was not representative of stomatal behavior during drought because *GPP* was not regulated only by stomatal closure but also by NSOL. Nevertheless, these results strengthen the increasing evidence that NSOL should be included in stomatal conductance/photosynthesis models to faithfully simulate both *GPP* and water fluxes in forest ecosystems.

Acknowledgments

The study has been performed thanks to the European Fluxes data base cluster. The authors would like to thank all the persons that contributed to this study. We would also like to thank all the financial support provided for sites. The financial support of the Research Foundation-Flanders (FWO) to the ICOS infrastructure is acknowledged. The BE-Vie was funded by the Service Public de Wallonie (Convention 1217769) which also gave us the opportunity for research at that site. The Czech sites were funded by the project SustES - Adaptation strategies for sustainable ecosystem services and food security under adverse environmental conditions“ (CZ.02.1.01/0.0/0.0/16_019/0000797).We would like to thank the University of Goettingen, Deutsche Forschungsgemeinschaft, and German Federal Ministry of Education and Research for funding the operation of DE-Hai. We thank the administration of the Hainich National Park for the opportunity for research in the National Park.Data from the Sorø beech forest site (DK-Sor) have been measured, evaluated and provided by Kim Pilegaard and Andreas Ibrom and the station team. The work was funded by the Technical University of Denmark (DTU), the Danish Research Council (DFF - 1323-00182), the Danish Ministry of higher Education and Science (5072-00008B) and the EU research infrastructure projects RINGO and ICOS.The data collected from the Salles ICOS station (FR-Bil) funded by INRA were obtained by C. Chipeaux (site manager), S. Lafont and D. Loustau (INRA, UMR ISPA). We acknowledge the support by successive European projects, by European regional development programs with the Region Lorraine, by GIP Ecofor and SOERE F-ORE-T, by ADEME, and by the INRA Department of Forest, Grassland and Freshwater Ecology (EFPA). Finally, We would also like to thank Carsten Gruening for his technical assistance.

References

1. Trenberth KE, Dai A, van der Schrier G, Jones PD, Barichivich J, Briffa KR, Sheffield J. 2014 Global warming and changes in drought. *Nat. Clim. Change* **4**, 17–22. (doi:10.1038/nclimate2067)

2. Vogel M, Zscheischler J, Wartenburger R, Dee D, Seneviratne S. 2019 Concurrent 2018 Hot Extremes Across Northern Hemisphere Due to Human-Induced Climate Change. *Earths Future* **7**, 692–703. (doi:10.1029/2019EF001189)

3. Toreti A *et al.* 2019 The Exceptional 2018 European Water Seesaw Calls for Action on Adaptation. *Earths Future* **7**, 652–663. (doi:10.1029/2019EF001170)

4. Ciais Ph *et al.* 2005 Europe-wide reduction in primary productivity caused by the heat and drought in 2003. *Nature* **437**, 529–533. (doi:10.1038/nature03972)

5. Granier A *et al.* 2007 Evidence for soil water control on carbon and water dynamics in European forests during the extremely dry year: 2003. *Agric. For. Meteorol.* **143**, 123–145. (doi:10.1016/j.agrformet.2006.12.004)

6. Reichstein M *et al.* 2007 Reduction of ecosystem productivity and respiration during the European summer 2003 climate anomaly: a joint flux tower, remote sensing and modelling analysis. *Glob. Change Biol.* **13**, 634–651. (doi:10.1111/j.1365-2486.2006.01224.x)

7. Sippel S, Reichstein M, Ma X, Mahecha MD, Lange H, Flach M, Frank D. 2018 Drought, Heat, and the Carbon Cycle: a Review. *Curr. Clim. Change Rep.* **4**, 266–286. (doi:10.1007/s40641-018-0103-4)

8. Reichstein M *et al.* 2002 Severe drought effects on ecosystem CO2 and H2O fluxes at three Mediterranean evergreen sites: revision of current hypotheses? *Glob. Change Biol.* **8**, 999–1017. (doi:10.1046/j.1365-2486.2002.00530.x)

9. Xu L, Baldocchi DD. 2003 Seasonal trends in photosynthetic parameters and stomatal conductance of blue oak (Quercus douglasii) under prolonged summer drought and high temperature. *Tree Physiol.* **23**, 865–877. (doi:10.1093/treephys/23.13.865)

10. Zhou S, Duursma RA, Medlyn BE, Kelly JWG, Prentice IC. 2013 How should we model plant responses to drought? An analysis of stomatal and non-stomatal responses to water stress. *Agric. For. Meteorol.* **182–183**, 204–214. (doi:10.1016/j.agrformet.2013.05.009)

11. Egea G, Verhoef A, Vidale PL. 2011 Towards an improved and more flexible representation of water stress in coupled photosynthesis–stomatal conductance models. *Agric. For. Meteorol.* **151**, 1370–1384. (doi:10.1016/j.agrformet.2011.05.019)

12. Migliavacca M *et al.* 2011 Semiempirical modeling of abiotic and biotic factors controlling ecosystem respiration across eddy covariance sites. *Glob. Change Biol.* **17**, 390–409. (doi:10.1111/j.1365-2486.2010.02243.x)

13. Reichstein M *et al.* 2003 Inverse modeling of seasonal drought effects on canopy CO2/H2O exchange in three Mediterranean ecosystems. *J. Geophys. Res. Atmospheres* **108**. (doi:10.1029/2003JD003430)

14. Knauer J, Zaehle S, Kauwe MGD, Bahar NHA, Evans JR, Medlyn BE, Reichstein M, Werner C. 2019 Effects of mesophyll conductance on vegetation responses to elevated CO2 concentrations in a land surface model. *Glob. Change Biol.* **25**, 1820–1838. (doi:10.1111/gcb.14604)

15. Keenan T, Sabate S, Gracia C. 2010 The importance of mesophyll conductance in regulating forest ecosystem productivity during drought periods. *Glob. Change Biol.* **16**, 1019–1034. (doi:10.1111/j.1365-2486.2009.02017.x)

16. Zhou S-X, Prentice IC, Medlyn BE. 2019 Bridging Drought Experiment and Modeling: Representing the Differential Sensitivities of Leaf Gas Exchange to Drought. *Front. Plant Sci.* **9**. (doi:10.3389/fpls.2018.01965)

17. Rogers A *et al.* 2017 A roadmap for improving the representation of photosynthesis in Earth system models. *New Phytol.* **213**, 22–42. (doi:10.1111/nph.14283)

18. Chaves MM, Flexas J, Pinheiro C. 2009 Photosynthesis under drought and salt stress: regulation mechanisms from whole plant to cell. *Ann. Bot.* **103**, 551–560. (doi:10.1093/aob/mcn125)

19. Medlyn BE *et al.* 2016 Using models to guide field experiments: a priori predictions for the CO2 response of a nutrient- and water-limited native Eucalypt woodland. *Glob. Change Biol.* **22**, 2834–2851. (doi:10.1111/gcb.13268)

20. Drake JE *et al.* 2017 Stomatal and non-stomatal limitations of photosynthesis for four tree species under drought: A comparison of model formulations. *Agric. For. Meteorol.* **247**, 454–466. (doi:10.1016/j.agrformet.2017.08.026)

21. Farquhar GD, von Caemmerer S, Berry JA. 1980 A biochemical model of photosynthetic CO2 assimilation in leaves of C3 species. *Planta* **149**, 78–90. (doi:10.1007/BF00386231)

22. Cowan IR, Farquhar GD. 1977 Stomatal function in relation to leaf metabolism and environment. *Symp. Soc. Exp. Biol.* **31**, 471–505.

23. Manzoni S, Vico G, Katul G, Fay PA, Polley W, Palmroth S, Porporato A. 2011 Optimizing stomatal conductance for maximum carbon gain under water stress: a meta-analysis across plant functional types and climates. *Funct. Ecol.* **25**, 456–467. (doi:10.1111/j.1365-2435.2010.01822.x)

24. Medlyn BE *et al.* 2011 Reconciling the optimal and empirical approaches to modelling stomatal conductance. *Glob. Change Biol.* **17**, 2134–2144. (doi:10.1111/j.1365-2486.2010.02375.x)

25. Ball JT, Woodrow IE, Berry JA. 1987 A Model Predicting Stomatal Conductance and its Contribution to the Control of Photosynthesis under Different Environmental Conditions. In *Progress in Photosynthesis Research: Volume 4 Proceedings of the VIIth International Congress on Photosynthesis Providence, Rhode Island, USA, August 10–15, 1986* (ed J Biggins), pp. 221–224. Dordrecht: Springer Netherlands. (doi:10.1007/978-94-017-0519-6_48)

26. Leuning R. 1995 A critical appraisal of a combined stomatal-photosynthesis model for C3 plants. *Plant Cell Environ.* **18**, 339–355. (doi:10.1111/j.1365-3040.1995.tb00370.x)

27. Knauer J *et al.* 2018 Towards physiologically meaningful water-use efficiency estimates from eddy covariance data. *Glob. Change Biol.* **24**, 694–710. (doi:10.1111/gcb.13893)

28. Lin Y-S *et al.* 2015 Optimal stomatal behaviour around the world. *Nat. Clim. Change* **5**, 459–464. (doi:10.1038/nclimate2550)

29. Medlyn BE *et al.* 2017 How do leaf and ecosystem measures of water-use efficiency compare? *New Phytol.* **216**, 758–770. (doi:10.1111/nph.14626)

30. Tarin T, Nolan RH, Medlyn BE, Cleverly J, Eamus D. 2019 Water-use efficiency in a semi-arid woodland with high rainfall variability. *Glob. Change Biol.* **n/a**. (doi:10.1111/gcb.14866)

31. Knauer J, El-Madany TS, Zaehle S, Migliavacca M. 2018 Bigleaf—An R package for the calculation of physical and physiological ecosystem properties from eddy covariance data. *PLOS ONE* **13**, e0201114. (doi:10.1371/journal.pone.0201114)

32. Monteith JL. 1965 Evaporation and environment. *Symp. Soc. Exp. Biol.* **19**, 205–234.

33. Kosugi Y, Takanashi S, Ueyama M, Ohkubo S, Tanaka H, Matsumoto K, Yoshifuji N, Ataka M, Sakabe A. 2013 Determination of the gas exchange phenology in an evergreen coniferous forest from 7 years of eddy covariance flux data using an extended big-leaf analysis. *Ecol. Res.* **28**, 373–385. (doi:10.1007/s11284-012-1019-4)

34. Granier A, Bréda N, Biron P, Villette S. 1999 A lumped water balance model to evaluate duration and intensity of drought constraints in forest stands. *Ecol. Model.* **116**, 269–283. (doi:10.1016/S0304-3800(98)00205-1)

35. Drought 2018 Team, ICOS Ecosystem Thematic Centre. 2019 Drought-2018 ecosystem eddy covariance flux product in FLUXNET-Archive format - release 2019-1 (Version 1.0). *ICOS Carbon Portal* (doi:https://doi.org/10.18160/PZDK-EF78)

36. Aubinet M *et al.* 2000 Estimates of the annual net carbon and water exchange of forests: the EUROFLUX methodology. *Adv. Ecol. Res.* **30**, 113–175.

37. Papale D *et al.* 2006 Towards a standardized processing of Net Ecosystem Exchange measured with eddy covariance technique: algorithms and uncertainty estimation. *Biogeosciences* **3**, 571–583.

38. Reichstein M *et al.* 2005 On the separation of net ecosystem exchange into assimilation and ecosystem respiration: review and improved algorithm. *Glob. Change Biol.* **11**, 1424–1439.

39. Héroult A, Lin Y-S, Bourne A, Medlyn BE, Ellsworth DS. 2013 Optimal stomatal conductance in relation to photosynthesis in climatically contrasting Eucalyptus species under drought. *Plant Cell Environ.* **36**, 262–274. (doi:10.1111/j.1365-3040.2012.02570.x)

40. Wang S, Yang Y, Trishchenko AP. 2009 Assessment of canopy stomatal conductance models using flux measurements. *Ecol. Model.* **220**, 2115–2118. (doi:10.1016/j.ecolmodel.2009.04.044)

41. Oosterbaan R, Sharma DP, Singh K, Rao KG. 1990 Crop production and soil salinity: evaluation of field data from India by segmented linear regression.

42. Bernacchi CJ, Singsaas EL, Pimentel C, Jr ARP, Long SP. 2001 Improved temperature response functions for models of Rubisco-limited photosynthesis. *Plant Cell Environ.* **24**, 253–259. (doi:10.1111/j.1365-3040.2001.00668.x)

43. Farquhar GD, Sharkey TD. 1982 Stomatal Conductance and Photosynthesis. *Annu. Rev. Plant Physiol.* **33**, 317–345. (doi:10.1146/annurev.pp.33.060182.001533)

44. Anderegg WRL *et al.* 2017 Plant water potential improves prediction of empirical stomatal models. *PLOS ONE* **12**, e0185481. (doi:10.1371/journal.pone.0185481)

45. Aubinet M, Hurdebise Q, Chopin H, Debacq A, De Ligne A, Heinesch B, Manise T, Vincke C. 2018 Inter-annual variability of Net Ecosystem Productivity for a temperate mixed forest: A predominance of carry-over effects? *Agric. For. Meteorol.* **262**, 340–353. (doi:10.1016/j.agrformet.2018.07.024)

46. Sellin A, Eensalu E, Niglas A. 2010 Is distribution of hydraulic constraints within tree crowns reflected in photosynthetic water-use efficiency? An example of Betula pendula. *Ecol. Res.* **25**, 173–183. (doi:10.1007/s11284-009-0641-2)

47. Kelliher FM, Leuning R, Raupach MR, Schulze E-D. 1995 Maximum conductances for evaporation from global vegetation types. *Agric. For. Meteorol.* **73**, 1–16. (doi:10.1016/0168-1923(94)02178-M)

48. Wilson K *et al.* 2002 Energy balance closure at FLUXNET sites. *Agric. For. Meteorol.* **113**, 223–243. (doi:10.1016/S0168-1923(02)00109-0)

49. Graf A *et al.* This issue Altered energy partitioning across terrestrial ecosystems in the European drought year 2018.

50. Keenan T, García R, Friend AD, Zaehle S, Gracia C, Sabate S. 2009 Improved understanding of drought controls on seasonal variation in Mediterranean forest canopy CO_2 and water fluxes through combined in situ measurements and ecosystem modelling. *Biogeosciences* **6**, 1423–1444. (doi:https://doi.org/10.5194/bg-6-1423-2009)

51. Chen B, Chen JM, Baldocchi DD, Liu Y, Wang S, Zheng T, Black TA, Croft H. 2019 Including soil water stress in process-based ecosystem models by scaling down maximum carboxylation rate using accumulated soil water deficit. *Agric. For. Meteorol.* **276–277**, 107649. (doi:10.1016/j.agrformet.2019.107649)

52. Op de Beeck M, Löw M, Deckmyn G, Ceulemans R. 2010 A comparison of photosynthesis-dependent stomatal models using twig cuvette field data for adult beech (Fagus sylvatica L.). *Agric. For. Meteorol.* **150**, 531–540. (doi:10.1016/j.agrformet.2010.01.018)

53. Hentschel R, Hommel R, Poschenrieder W, Grote R, Holst J, Biernath C, Gessler A, Priesack E. 2016 Stomatal conductance and intrinsic water use efficiency in the drought year 2003: a case study of European beech. *Trees* **30**, 153–174. (doi:10.1007/s00468-015-1284-2)

54. Galmés J, Medrano H, Flexas J. 2007 Photosynthetic limitations in response to water stress and recovery in Mediterranean plants with different growth forms. *New Phytol.* **175**, 81–93. (doi:10.1111/j.1469-8137.2007.02087.x)

55. Keenan T, Sabate S, Gracia C. 2010 Soil water stress and coupled photosynthesis–conductance models: Bridging the gap between conflicting reports on the relative roles of stomatal, mesophyll conductance and biochemical limitations to photosynthesis. *Agric. For. Meteorol.* **150**, 443–453. (doi:10.1016/j.agrformet.2010.01.008)

56. Flexas J, Bota J, Loreto F, Cornic G, Sharkey TD. 2004 Diffusive and Metabolic Limitations to Photosynthesis under Drought and Salinity in C3 Plants. *Plant Biol.* **6**, 269–279. (doi:10.1055/s-2004-820867)

57. Flexas J *et al.* 2012 Mesophyll diffusion conductance to CO2: An unappreciated central player in photosynthesis. *Plant Sci.* **193–194**, 70–84. (doi:10.1016/j.plantsci.2012.05.009)

58. Lawlor DW, Tezara W. 2009 Causes of decreased photosynthetic rate and metabolic capacity in water-deficient leaf cells: a critical evaluation of mechanisms and integration of processes. *Ann. Bot.* **103**, 561–579. (doi:10.1093/aob/mcn244)

59. Mäkelä A, Berninger F, Hari P. 1996 Optimal Control of Gas Exchange during Drought: Theoretical Analysis. *Ann. Bot.* **77**, 461–468. (doi:10.1006/anbo.1996.0056)

60. Buckley TN. 2019 How do stomata respond to water status? *New Phytol.* **224**, 21–36. (doi:10.1111/nph.15899)

61. Flexas J, Medrano H. 2002 Drought-inhibition of photosynthesis in C3 plants: stomatal and non-stomatal limitations revisited. *Ann. Bot.* **89**, 183–189. (doi:10.1093/aob/mcf027)

62. Tuzet A, Perrier A, Leuning R. 2003 A coupled model of stomatal conductance, photosynthesis and transpiration. *Plant Cell Environ.* **26**, 1097–1116. (doi:10.1046/j.1365-3040.2003.01035.x)

63. Tuzet A, Granier A, Betsch P, Peiffer M, Perrier A. 2017 Modelling hydraulic functioning of an adult beech stand under non-limiting soil water and severe drought condition. *Ecol. Model.* **348**, 56–77. (doi:10.1016/j.ecolmodel.2017.01.007)

64. Dewar R, Mauranen A, Mäkelä A, Hölttä T, Medlyn B, Vesala T. 2018 New insights into the covariation of stomatal, mesophyll and hydraulic conductances from optimization models incorporating nonstomatal limitations to photosynthesis. *New Phytol.* **217**, 571–585. (doi:10.1111/nph.14848)

65. Sperry JS, Wang Y, Wolfe BT, Mackay DS, Anderegg WRL, McDowell NG, Pockman WT. 2016 Pragmatic hydraulic theory predicts stomatal responses to climatic water deficits. *New Phytol.* **212**, 577–589. (doi:10.1111/nph.14059)

66. Gimeno TE, Saavedra N, Ogée J, Medlyn BE, Wingate L. 2019 A novel optimization approach incorporating non-stomatal limitations predicts stomatal behaviour in species from six plant functional types. *J. Exp. Bot.* **70**, 1639–1651. (doi:10.1093/jxb/erz020)

67. Gielen B, De Vos B, Campioli M, Neirynck J, Papale D, Verstraeten A, Ceulemans R, Janssens IA. 2013 Biometric and eddy covariance-based assessment of decadal carbon sequestration of a temperate Scots pine forest. *Agric. For. Meteorol.* **174–175**, 135–143. (doi:10.1016/j.agrformet.2013.02.008)

68. Acosta M, Darenova E, Dušek J, Pavelka M. 2017 Soil carbon dioxide fluxes in a mixed floodplain forest in the Czech Republic. *Eur. J. Soil Biol.* **82**, 35–42. (doi:10.1016/j.ejsobi.2017.08.006)

69. McGloin R, Šigut L, Havránková K, Dušek J, Pavelka M, Sedlák P. 2018 Energy balance closure at a variety of ecosystems in Central Europe with contrasting topographies. *Agric. For. Meteorol.* **248**, 418–431. (doi:10.1016/j.agrformet.2017.10.003)

70. Krupková L, Havránková K, Krejza J, Sedlák P, Marek MV. 2019 Impact of water scarcity on spruce and beech forests. *J. For. Res.* **30**, 899–909. (doi:10.1007/s11676-018-0642-5)

71. Schrumpf M, Kaiser K, Guggenberger G, Persson T, Kögel-Knabner I, Schulze E-D. 2013 Storage and stability of organic carbon in soils as related to depth, occlusion within aggregates, and attachment to minerals. *Biogeosciences* **10**, 1675–1691. (doi:https://doi.org/10.5194/bg-10-1675-2013)

72. Herbst M, Mund M, Tamrakar R, Knohl A. 2015 Differences in carbon uptake and water use between a managed and an unmanaged beech forest in central Germany. *For. Ecol. Manag.* **355**, 101–108. (doi:10.1016/j.foreco.2015.05.034)

73. Pilegaard K, Ibrom A, Courtney MS, Hummelshøj P, Jensen NO. 2011 Increasing net CO2 uptake by a Danish beech forest during the period from 1996 to 2009. *Agric. For. Meteorol.* **151**, 934–946. (doi:10.1016/j.agrformet.2011.02.013)

74. Moreaux V, Lamaud E, Bosc A, Bonnefond J-M, Medlyn BE, Loustau D. 2011 Paired comparison of water, energy and carbon exchanges over two young maritime pine stands (Pinus pinaster Ait.): effects of thinning and weeding in the early stage of tree growth. *Tree Physiol.* **31**, 903–921. (doi:10.1093/treephys/tpr048)

75. Granier A, Bréda N, Longdoz B, Gross P, Ngao J. 2008 Ten years of fluxes and stand growth in a young beech forest at Hesse, North-eastern France. *Ann. For. Sci.* **65**, 1. (doi:10.1051/forest:2008052)

Tables

Table 1: Main characteristics of the flux tower sites included in this study. The LAI corresponds to the maximum LAI typically observed at the sites.

Site ID	Country	Latitute	Longitude	Dominating species	LAI	Soil texture	Rooting depth	ref
					$m^2\ m^{-2}$		m	
BE-Bra	Belgium	51.308	4.52	*Pinus syvlestris*	3	sand	1	[67]
BE-Vie	Belgium	50.305	5.998	*Fagus sylvatica/Pseudotsuga menziesii*	5	silty clay loam	1.4	[45]
CZ-Lnz	Czechia	48.682	16.946	*Quercus robur/Fraxinus angustifolia/Carpinus betulus/Tilia cordata*	6.5	sandy loam	1.2	[68]
CZ-Raj	Czechia	49.444	16.697	*Picea abies*	5	sandy loam	0.7	[69]
CZ-Stn	Czechia	49.036	17.97	*Fagus sylvatica*	5.5	sandy loam	0.7	[70]
DE-Hai	Germany	51.0792	10.453	*Fagus sylvatica*	6	clay loam	0.7	[71,72]
DK-Sor	Denmark	55.486	11.645	*Fagus sylvatica*	5	sandy clay loam	1	[73]
FR-Bil	France	44.494	-0.956	*Pinus pinaster*	2.5	sand	1.1	[74]
FR-Hes	France	48.674	7.065	*Fagus sylvatica*	6.5	silty clay loam	1.6	[75]
IT-Sr2	Italy	43.732	10.291	*Pinus pinea*	2.5	sand	1.2	

Table 2: Maximum extractable water (*EW*), minimum observed *REW* in 2018 during the growing season, $REW_{b,VCMAX}$ and $REW_{b,G1}$ (*REW* break points for $V_{CMAX,APP}$ and G_1 respectively) given with 95% confidence intervals. $V_{CMAX,APP}$* and G_1* ($V_{CMAX,APP}$ and G_1 values in unstressed conditions) given with 95% confidence intervals. pvalue are given for the F test comparing the segmented mode (3 parameters) to the linear model (2 parameters).

Site ID	EW	min *REW*	$V_{CMAX,APP}$*	$REW_{b,VCMAX}$	pvalue	G_1*	$REW_{b,G1}$	pvalue
	mm	--	$\mu mol\ m^{-2}\ s^{-1}$	--	--	$kPa^{-0.5}$	--	--
BE-Bra	133	0.30	71 ± 5	0.37 ± 0.03	<0.01**	3.0 ± 0.2	--	0.07
BE-Vie	215	0.19	75 ± 4	--	1	1.8 ± 0.1	--	0.18
CZ-Lnz	241	0.49	154 ± 10	--	1	1.7 ± 0.2	--	1
CZ-Raj	92	0.07	70 ± 6	0.39 ± 0.11	<0.01**	1.6 ± 0.8	--	1
CZ-Stn	236	0.46	154 ± 10	--	0.11	2.2 ± 0.3	--	1
DE-Hai	143	0.00	87 ± 10	0.38 ± 0.07	<0.001***	1.6 ± 0.2	0.16 ± 0.06	<0.001***
DK-Sor	176	0.25	133 ± 8	0.85 ± 0.09	<0.05*	2.2 ± 0.2	--	1
FR-Bil	159	0.08	89 ± 7	0.40 ± 0.12	<0.001***	5.1 ± 0.4	--	1
FR-Hes	338	0.33	121 ± 13	0.48 ± 0.10	<0.05*	1.9 ± 0.5	--	1
IT-Sr2	108	0.08	92 ± 4	--	0.21	2.6 ± 0.2	--	0.13

Figures

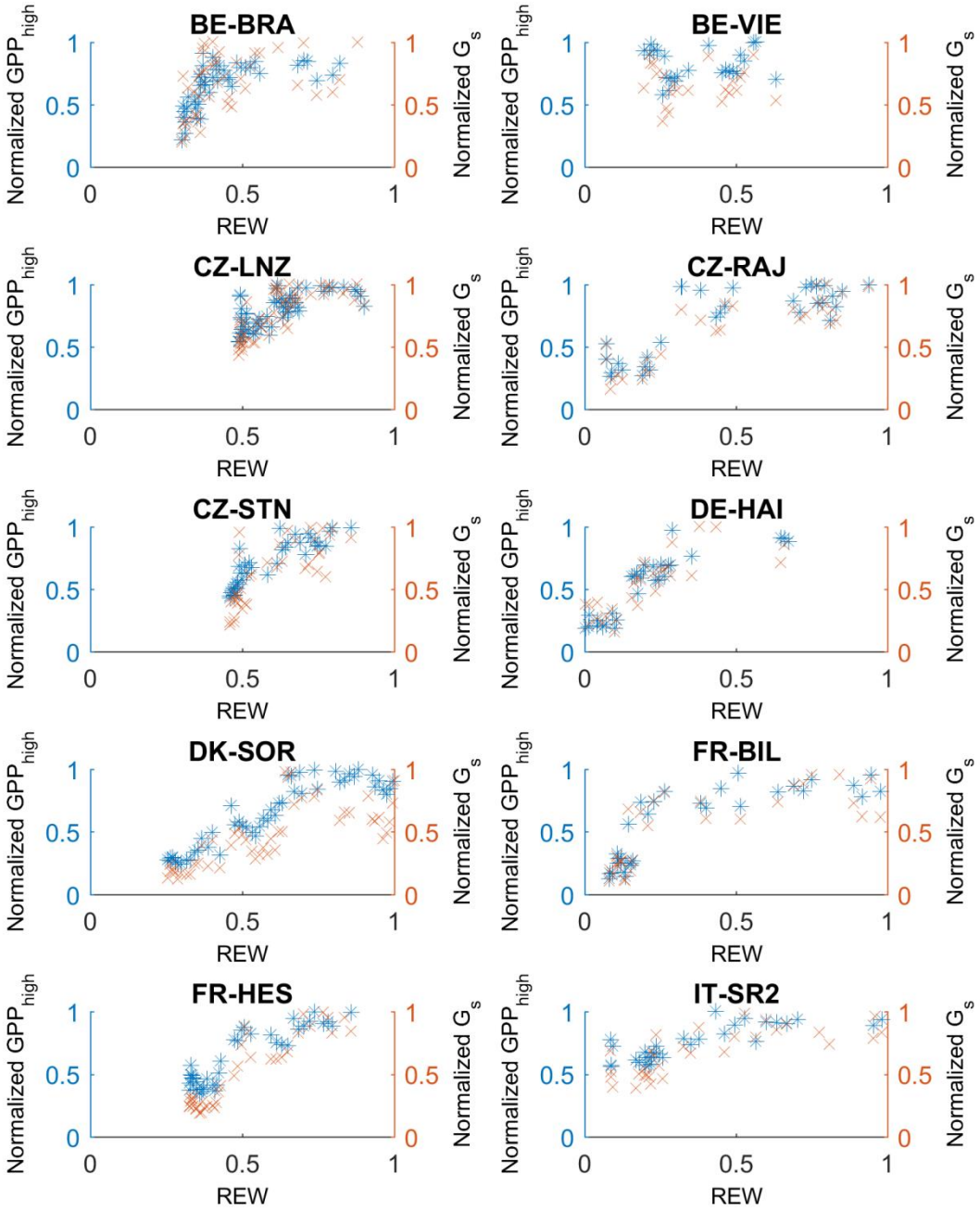

Figure 1: Dependence of GPP_{high} (blue, left axis) and G_s at high radiation (Rg>500, red, right axis) normalized by their maximum value on *REW* for each site.

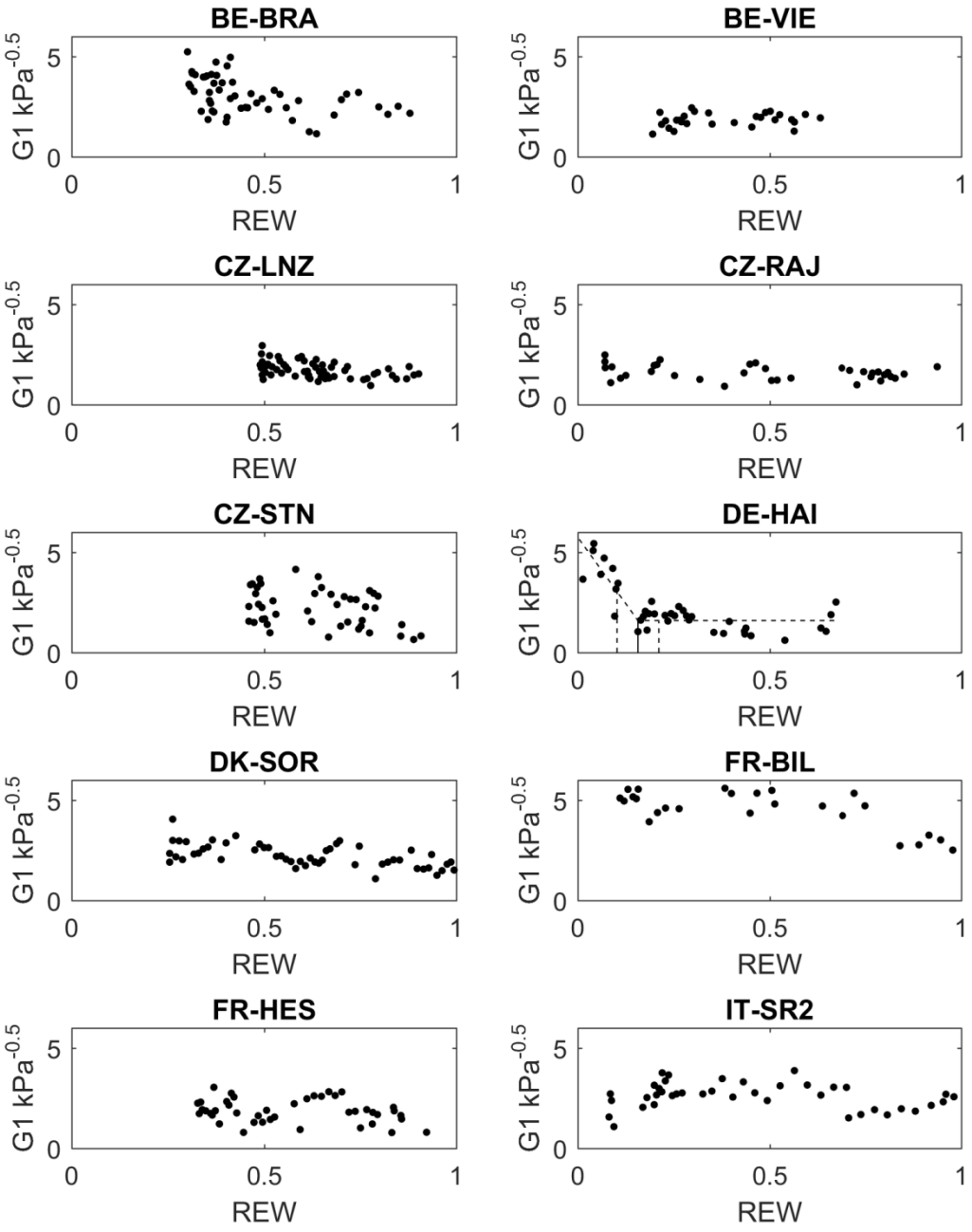

Figure 2: Dependence of G_1 on *REW* for each site. $REW_{B,G1}$ are marked by a vertical solid line with 95% confidence intervals (dashed vertical lines). Regression lines are only shown when F-test pvalues (comparison with linear regression) were smaller than 0.05.

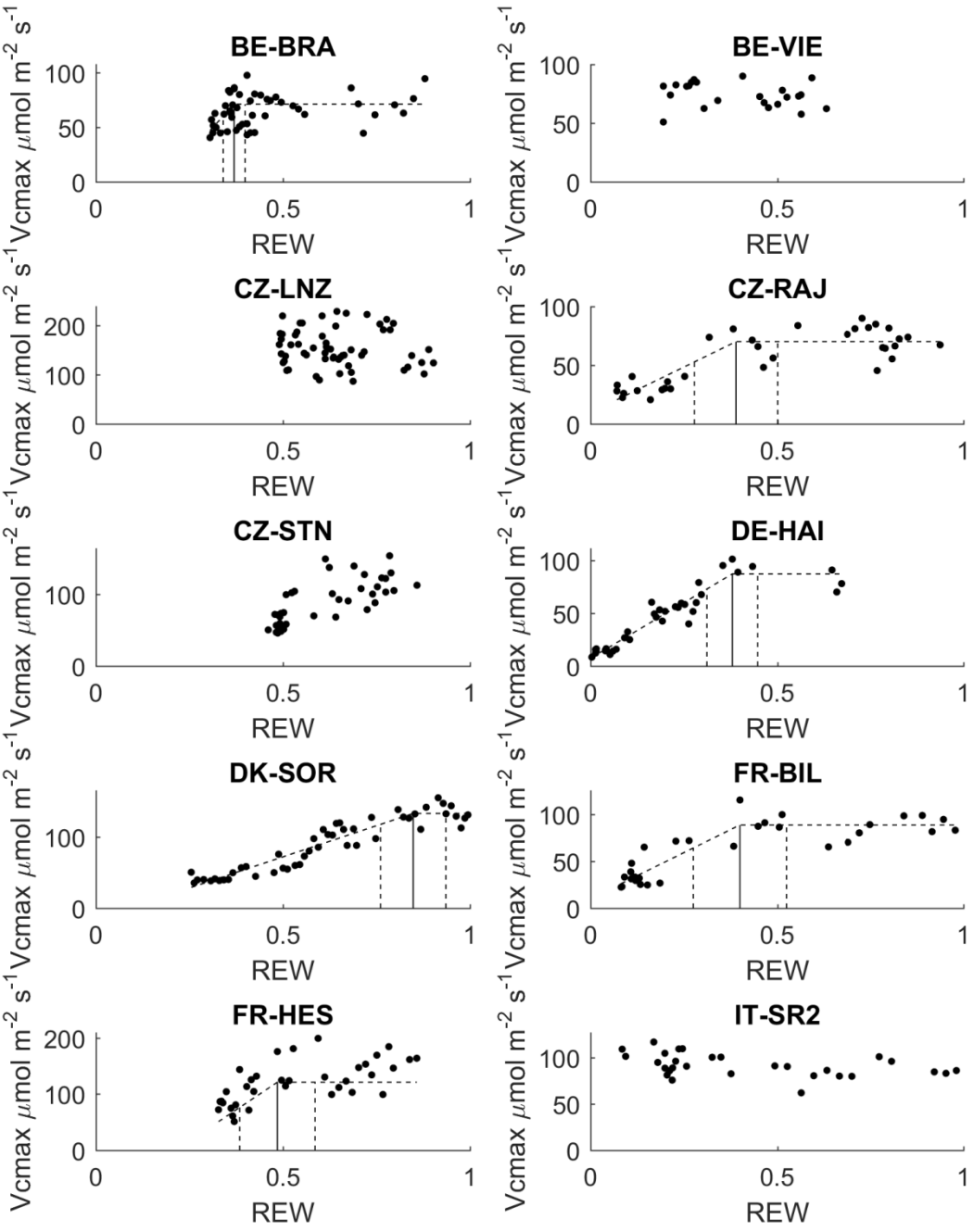

Figure 3: Dependence of $V_{CMAX,APP}$ normalized at 25°C on *REW* for each site. $REW_{B,VCMAX}$ are marked by a vertical solid line with 95% confidence intervals (dashed vertical lines). Regression lines are only shown when F-test pvalues (comparison with linear regression) were smaller than 0.05.

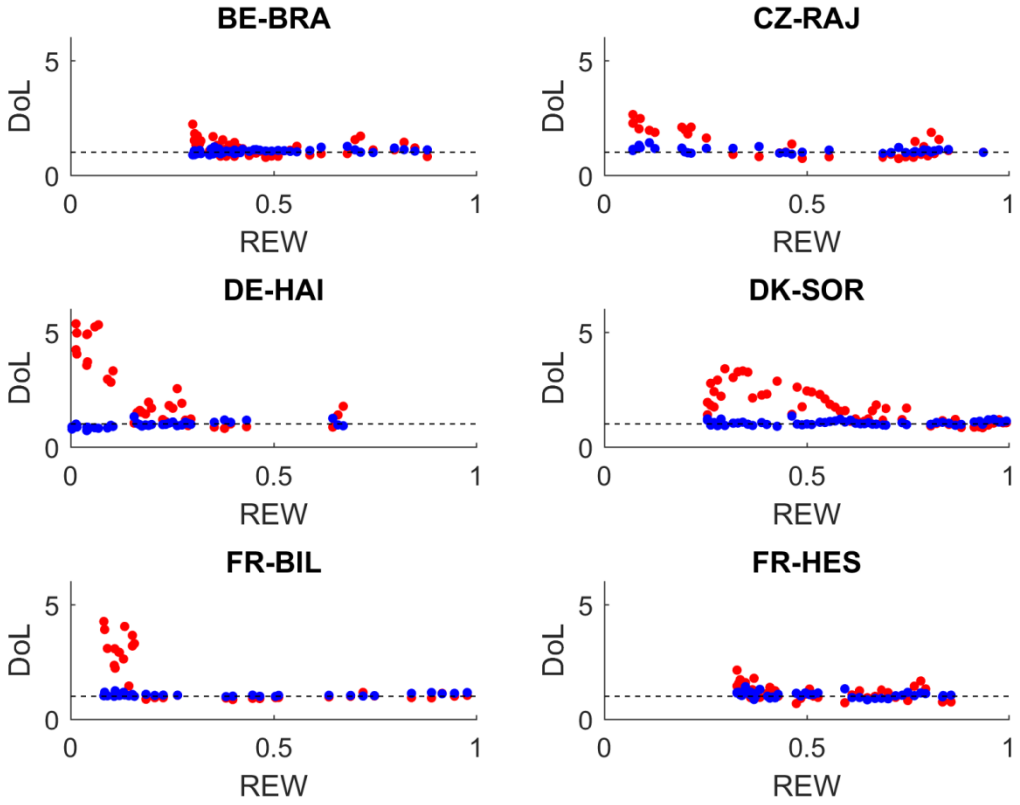

Figure 4: Degree of limitation (DoL) by both SOL and NSOL. The degree of limitation was computed as the ratio of modelled *GPP* on measured *GPP* at high radiation. Modelled *GPP* was computed by using either fixed $V_{CMAX,APP}^{*}$ (red points, NSOL) and varying G_1 or fixed G_1* and observed $V_{CMAX,APP}$ (blue points, SOL).